energies

MDPI

Article

Solar-Driven Sorption System for Seasonal Heat Storage under Optimal Control: Study for Different Climatic Zones

Alicia Crespo [1], Cèsar Fernández [1], Alvaro de Gracia [2] and Andrea Frazzica [3,*]

[1] GREiA Research Group, University of Lleida, Pere de Cabrera s/n, 25001 Lleida, Spain; alicia.crespo@udl.cat (A.C.); cesar.fernandez@udl.cat (C.F.)
[2] IT4S Research Group, Universitat de Lleida, Pere de Cabrera s/n, 25001 Lleida, Spain; alvaro.degracia@udl.cat
[3] Institito di Tecnologie Avanzate per l'Energia "Nicola Giordano", CNR-ITAE, 98126 Messina, Italy
* Correspondence: andrea.frazzica@itae.cnr.it

Abstract: Solar thermal energy coupled to a seasonal sorption storage system stands as an alternative to fossil fuels to supply residential thermal energy demand in climates where solar energy availability is high in summer and low in winter, matching with a high space heating demand. Sorption storage systems usually have a high dependency on weather conditions (ambient temperature and solar irradiation). Therefore, in this study, the technical performance of a solar-driven seasonal sorption storage system, using an innovative composite sorbent and water as working fluid, was studied under three European climates, represented by: Paris, Munich, and Stockholm. All scenarios analyses were simulation-based under optimal system control, which allowed to maximize the system competitiveness by minimizing the system operational costs. The optimal scenarios profit from just 91, 82 and 76% of the total sorption system capacity, for Paris, Munich, and Stockholm, respectively. That means that an optimal control can identify the optimal sorption storage size for each location and avoid oversizing in future systems, which furthermore involves higher investment costs. The best coefficient of performance was obtained for Stockholm (0.31), despite having the coldest climate. The sorption system was able to work at minimum temperatures of −15 °C, showing independence from ambient temperature during its discharge. In conclusion, a seasonal sorption system based on selective water materials is suitable to be integrated into a single-family house in climates of central and northern Europe as long as an optimal control based on weather conditions, thermal demand, and system state is considered.

Keywords: water-based sorption storage; seasonal storage; simulations; control optimization; climatic zones

Citation: Crespo, A.; Fernández, C.; de Gracia, A.; Frazzica, A. Solar-Driven Sorption System for Seasonal Heat Storage under Optimal Control: Study for Different Climatic Zones. *Energies* **2022**, *15*, 5604. https://doi.org/10.3390/en15155604

Academic Editor: Antonio Rosato

Received: 1 July 2022
Accepted: 28 July 2022
Published: 2 August 2022

1. Introduction

The objective of the Paris Agreement reached at COP21 [1] was to limit global warming "well-below 2 °C" above pre-industrial levels. To reach this challenging goal, a global energy transition where clean energies take a centre stage is fundamental. According to the International Energy Agency (IEA) [2], heat is the largest energy end-use, accounting for half of the global final energy consumption. Focusing on the residential sector, the thermal demand accounts for 46% of the global heat consumption [3]. Renewable heat sources, such as solar energy, could contribute to supply a large percentage of that global heat consumption, leading us to a decarbonize energy matrix. Nevertheless, modern renewables account for only 11% of global heat supply today [2]. In particular, solar collectors coupled to seasonal thermal energy storage makes it possible to store solar heat during summer and release it in winter, when the solar resource availability is low and the space heating demands in the households are high.

Yang et al. [4] reviewed six types (see Figure 1) of seasonal thermal energy storage systems from a techno-economic perspective. According to the authors, latent and thermochemical storage exhibit the best technical performance. Latent heat storage can be

considered a good candidate due to its high energy density and its ability to supply heat at a nearly constant temperature. Nevertheless, it presents several disadvantages, among which stand out the lack of thermal stability, the potential degradation [4], and the thermal losses between summer and winter seasons. Thermochemical storage based on the sorption process stands as a very promising solution for seasonal TES since it presents zero thermal losses during the storage period, which is a crucial requirement for long-term seasonal storage. Furthermore, sorption storage also presents high energy densities at material level. Nevertheless, thermochemical storage requires further research at the material, system, and operational level.

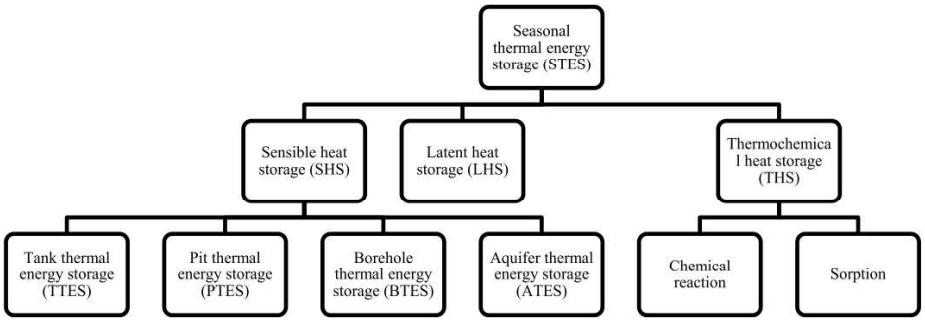

Figure 1. Schematic representation of the nodes of the TES [4].

The sorption storage process is based on the reaction between a sorbate, sometimes referred to as working fluid (e.g., water, ammonia, alcohols) and a sorbent, which can be either a solid or a liquid solution. The interaction between the two components is either physical or through weak chemical reactions [5]. For this reason, sorption processes are suitable for residential applications since the reversible reaction can be driven by low-medium charging temperatures (i.e., 80–120 °C) [6], which can be provided by commercial non-concentrating solar thermal technologies.

Several authors have already studied ammonia-based sorption storage systems for space heating applications [7–9]. This type of sorption systems has the advantages of high-operation pressure and low freezing point of liquid ammonia compared to water-based sorption storage [10]. Nevertheless, the toxicity of ammonia can hinder its commercial implementation in the residential sector. Sorption TES based on a water sorbent is a more environmentally friendly solution for households. Some authors have studied its thermal performance for heating generation at a pilot scale [11–15]. Most of the studies analysed or optimized system parameters such as outlet temperature, mass transfer, or energy density under well-defined testing conditions. Nevertheless, an extrapolation from the prototypes or small-scale systems to full-scale systems coupled to the dynamics of a dwelling thermal demand and weather conditions requires attention from the scientific community. Sorption storage systems require a low temperature heat source (above 0 °C for water-based ones) to assist the evaporator. During intermediate season or warm winter days, ambient air can be used as heat source. In summer, ambient air can also be used as heat sink by the condenser. Moreover, when solar heat is also used as heat source, the system dependency on weather conditions is higher. Therefore, to really understand the impact of weather conditions and optimize the thermal performance of sorption heat storage systems at a real scale, a study of the system coupled to a dwelling thermal demand subjected to different climates must be carried out. Few studies analysed the impact of different climatic conditions on seasonal sorption systems. Ma et al. [16] studied the feasibility of using sensible, latent, and thermochemical storage technologies to supply the space heating (SH) and domestic hot water (DHW) demand of domestic dwellings in eight representative cities of the UK. Nevertheless, the authors did not deepen into the performance of the thermochemical storage system. Engel et al. [17] performed a detailed simulation of a solar-driven water-based sorption storage system. The solar fraction of the sorption system was analysed for different locations under different building load profiles

(15, 30, 60 and 100 kWh/m^3). All simulations were performed with one set of parameters and system dimensions. However, the control settings were not optimal for all the locations and heat demands. Indeed, the authors reported that for some locations, the sorption storages were considerably oversized and that it could have been avoided by adjusting the control strategy. On a yearly basis, Mlakar et al. [18] simulated the performance of a thermochemical storage that supplied space heating to a building located in two Slovenian locations: Ljubljana and Portorož. The software tools: TRNSYS and MS Excel, were used to simulate the system. The results showed that the simulation was highly dependent on the climatic conditions of each geographical location. Furthermore, the study showed that thermochemical storage can achieve 100% of coverage for heat demand of a building. Jiang et al. [7] analysed a hybrid ammonia-based sorption seasonal storage driven by PVT collectors under three different severe cold regions. The authors concluded that the hybrid technology could be promising to solve the heating issues in severe cold regions during winter. Frazzica et al. [19] proposed a new unified methodology for the optimization of the seasonal sorption storage sizing, depending on building constraints, weather conditions, and solar thermal technologies. The method was based on energy balance considerations and climatic analysis, thus providing a tool for the sizing but not focusing on any optimized operation of the technology.

As N'Tsoukpoe et al. [20] reported, seasonal sorption storage systems are subjected to significant sensible thermal losses, which in turn impact in the COP of the system, which represents the ratio between the energy discharged in winter to the energy stored in summer. An optimal control of the system can contribute to minimize the heat losses between two consecutive charges and discharges by identifying which system states and weather conditions benefit its performance. Furthermore, other studies [18] have already proved the dependency of sorption storage systems on climatic conditions. Therefore, in this study, the performance of a seasonal sorption storage composed by an innovative asymmetric heat exchanger (reactor) [21] filled by a novel selective water sorbent (SWS) [22] was studied under different climatic conditions. Moreover, as Engel et al. [17] reported, adjusting the control strategy for each location can avoid oversizing. Nevertheless, to the authors knowledge, the analysis of a solar-driven sorption seasonal sorption system subjected to different climate conditions, each of them operated under detailed optimal control, has not been studied before. Hence, in this study, in addition to analysing the impact of different weather conditions on the thermal performance of a sorption thermal energy storage (STES) system, the optimal control scenario for each location was identified and analysed. The seasonal energy system which supplied SH and DHW to a single-family house was studied through numerical simulations under three different locations: Paris, Munich, and Stockholm. The system was operated with a rule-based control (RBC) strategy, which was optimized for the corresponding thermal demand, solar irradiation, ambient temperature, and system conditions of each location. The authors of the present study are aware of the actual limitations of long-term solar heat storage for household application. Precisely for that, we think that further research, especially in the design optimization, system integration, and control, is necessary. The present study will help to open a better scenario with respect to the integration of seasonal sorption systems into households.

This study is divided as follows. Section 2 describes the methodology followed. It includes a description of the system and its operation and a description of the numerical models. An explanation of the three case studies and their control optimization methodology is also included in Section 2. Sections 3 and 4 present the results and conclusions, respectively.

2. Methodology

2.1. Solar-Driven Seasonal Sorption System

In this study, the impact of climatic conditions on the performance of a solar-driven seasonal water-based sorption system that supplied domestic hot water (DHW) and space heating (SH) to a single-family house is analysed. Evacuated tube collectors supplied heat to either a stratified water tank, a seasonal sorption storage system, or a low temperature

heat source (LTHS), depending on the season, solar irradiation, ambient temperature, and the state variables. During the summer season (from April to end of September), solar heat with high enthalpy was used to charge the sorption storage system at regeneration temperatures around 90 °C. The sorption storage was composed by 20 modules of a composite material which consisted of LiCl embedded in a Silica gel matrix [22] (known as selective water sorbent (SWS)). The sorption storage used ambient air as environmental sink to the condenser during its charging process. In addition to charge the sorption modules in summer, solar heat at lower enthalpy was used to charge the stratified water tank for DHW application (65 °C), and to a lower extent for SH during the intermediate season. DHW and SH were supplied from the upper and middle part of the water tank, respectively (see Figure 2), when needed. A back-up gas boiler assisted the system when the temperature in the stratified water tank was below the corresponding set point.

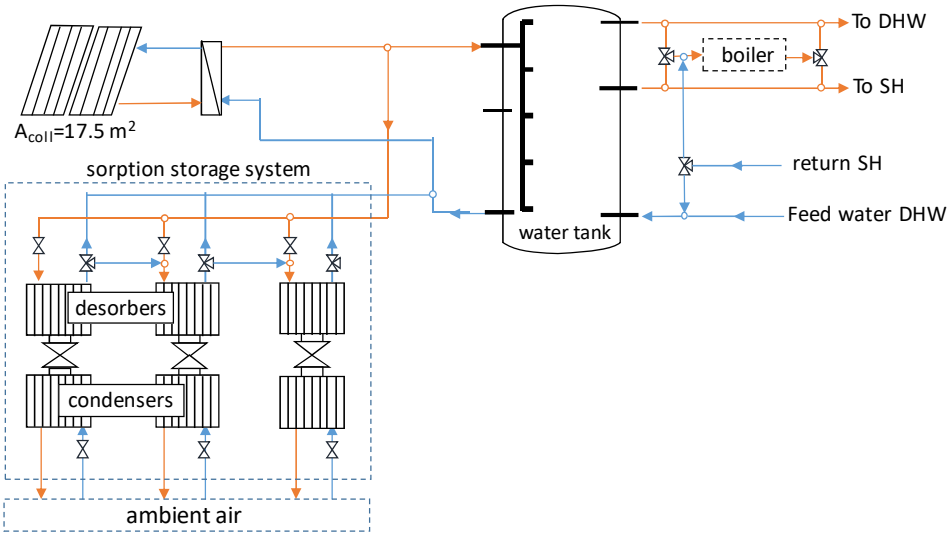

Figure 2. Schematic of the system for summer configuration.

During winter (from October to end of March), the solar energy availability was low and the SH heating demand was high. Therefore, when there was SH demand and the middle part of the water tank was below the set-point, heat of sorption was discharged from the sorption modules to the stratified water tank. The sorption storage was discharged at a composite temperature of 35 °C. The SH demand set-point was dependent of the ambient temperature, according the floor SH distribution system [23]. Due to the working cycle of the selected composite material, radiant floor heating was selected, which works at supply temperature ranging from 25 to 35 °C, depending on the energy efficiency of the building's envelope and outdoor ambient temperature.

Water-based sorption storage systems require a low temperature heat source that supplies heat above 0 °C (from 5 to 15 °C in this case) to the evaporator during the discharging process. In the proposed system, to avoid full dependency of the sorption system to the ambient temperature, a low temperature heat source charged by solar energy at low enthalpy was implemented (see Figure 3). Additionally, if the ambient temperatures where high enough, ambient heat was used to assist the evaporator.

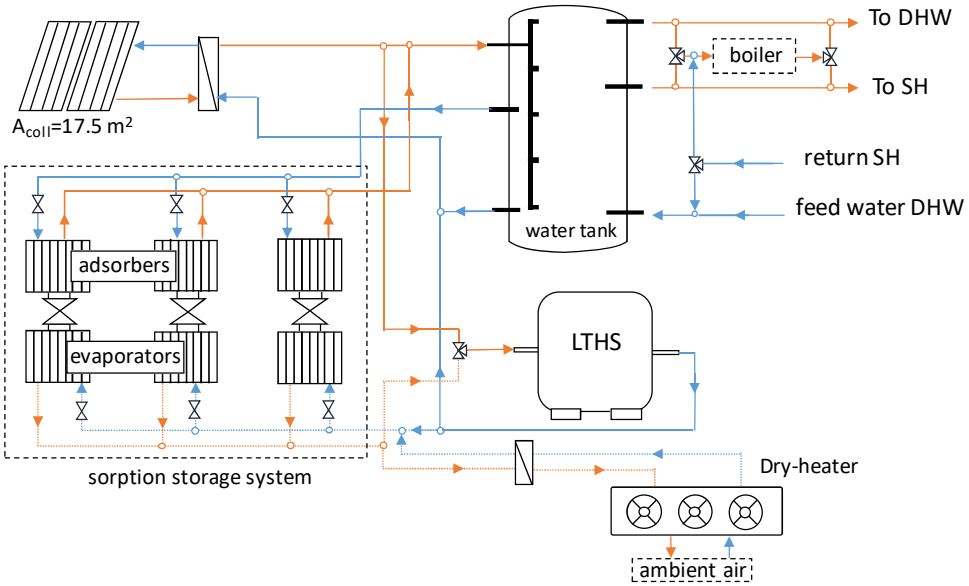

Figure 3. Schematic of the system for winter configuration.

As happened in summer, during winter days with relatively high solar irradiation the stratified water tank was charged with solar heat to supply DHW and SH needs. SH demand was supplied directly by the stratified tank, with assistance from the back-up boiler or working in close loop when the temperatures in the middle part of the water tank were below 20 °C (lower than the SH return temperature). When the gas boiler was required by both DHW and SH, the DHW was prioritized, which means that, during the corresponding time period (usually 15 min), the system was not accomplishing the user comfort.

2.2. System Simulation

Numerical models and performance maps implemented in Python [24] were used to simulate the thermal performance of the different subcomponents of the system. Once all models described below were implemented, their interconnection and coupling with the transient weather data and thermal demand was carried out also in Python. A time-step of 15 min was used for the simulations. The same subsystems design parameters (size, mass flow rate, etc.), which were derived from the technical report of a European project [25], were considered to analyse the different climatic locations.

Solar collectors

A 17.5 m^2 solar field composed by evacuated tube collectors [26] was used in the simulations. The generic equation of the thermal performance of a solar collector presented by Duffie and Beckman [27] can be expressed based on the collector overall efficiency ($\eta_{overall}$), as shown in Equations (1) and (2):

$$IAM\ E_G\ A_{col}\ \eta_{overall} = \dot{m}_{col}\ C_p(T_{out,col} - T_{in,col}) \quad (1)$$

$$\eta_{overall} = a_0 - a_1\frac{T_{avg,col} - T_{amb}}{E_G} - a_2\frac{\left(T_{avg,col} - T_{amb}\right)^2}{E_G} \quad (2)$$

where *IAM* is the incidence angle modifier, E_G is the solar global irradiation in the titled surface, *Acol* is the collector area, $\dot{m}_{col}$ is the collector mass flow rate, $T_{out,col}$, $T_{in,col}$ and $T_{avg,col}$ are the outlet, inlet, and average collector temperatures, respectively, a_0 is the collector optical efficiency and a_1 and a_2 are the first and second order collector efficiencies, respectively. Water-glycol with a specific heat (*Cp*) of 3.9 kJ/kg·K was considered as HTF in the simulations. The optimal and thermal properties of the collector are shown in Table 1.

Table 1. Optical and thermal properties of the solar collector used in the simulations.

Parameter	Value	Parameter	Value
a_0	0.559 [28]	Mass flow range (kg/h)	300–1000
a_1 (W/m^{2}K)	1.485 [28]	Diffuse IAM	1.314 [28]
a_2 (W/m^{2}K^2)	0.002 [28]	Maximum pressure (bar)	10 [29]

The evacuated tube collector model was validated against results reported by Ayompe et al. [30]. The deviation between the reference and the present model was lower than 1% in terms of the collector outlet temperature average relative error.

Stratified water tank

A constant volume stratified water tank was used in the simulations to store solar heat and supply it for DHW and SH. A 1D numerical model which considered thermal losses to the ambient, conduction between adjacent nodes, and mass exchange between nodes was used. The model was based on the finite control volume method, i.e., every control volume had uniform thermal properties. The set of equations, solved with an explicit scheme, used to model the heat transfer in the water tank were presented by Rodriguez-Hidalgo et al. [31].

A sketch of the stratified tank used in the simulation is shown in Figure 4. The original water tank (as shown in Figure 4) did not have a perfect cylindrical shape. An equivalent height considering a perfect cylindrical shape was considered to allow for a structured grid in the discretization of the domain. The model, simulated using 33 control volumes (nodes), was validated against experiments performed at the laboratory of GREiA at the University of Lleida. For the validation, just five nodes along the tank were considered, obtaining an average error of 2.1%. More information about the set-up and the water tank can be found at [32].

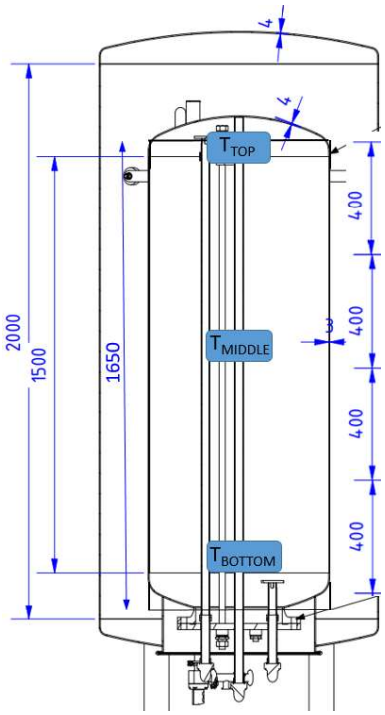

Figure 4. Sketch of the stratified tank [33] used in the simulations.

The control policy of the system required the instant temperature values at the top and middle part of the water tank, which corresponded to the regions intended for DHW and SH, respectively. That means that, out of the 33 control volumes, just 3 of them (simulating

3 sensors) located at the top, middle, and bottom part of the stratified tank were used in the simulations as control parameters. The parameters of the stratified water tank used in the simulations are presented in Table 2.

Table 2. Parameters of the stratified water tank used in the simulations.

Parameter	Value	Parameter	Value
Top heat losses coefficient [W/m^{2}K]	0.32 [32]	Height [m]	1.65
Edges heat losses coefficient [W/m^{2}K]	0.38 [32]	Volume [m^3]	1
Bottom heat losses coefficient [W/m^{2}K]	0.002 [32]	HTF thermal conductivity [W/m·K]	10

Sorption storage tank

Some studies tested prototypes of sorption reactors at laboratory or pilot-scale for TES applications using solid pure adsorbents or composite materials [12–15,34]. Scaling up the reactors from laboratory scale or pilot scale to real scale entails design, manufacturing, and testing challenges. To the authors knowledge, just one study [12] analysed a closed sorption storage system at real-scale for household SH application using composite materials, as the one presented in this study. Studies about the thermal performance of real-scale reactors of both open and closed systems is missing in the literature. For this reason, Hu et al. [35] presented a set of ratios to scale up an open zeolite sorption TES from a pilot to full-scale, which theoretically ensured similar geometry, dynamics, sorption-kinetics, and thermal performance. In this study, the thermal performance of the closed sorption TES system under study was obtained from the scaling up of experimental tests. The experimental measurements of a novel lab-scale adsorber (asymmetric plate heat exchanger) reported by Mikhaeil et al. [21] together with the kinetic characterization [36] of the water adsorbent material used in this study (LiCl/silica gel) were scaled up to obtain the performance maps of 100 kg SWS sorption module. A detailed sketch of a sorption module is shown in Figure 5 (temperatures correspond to charging process).

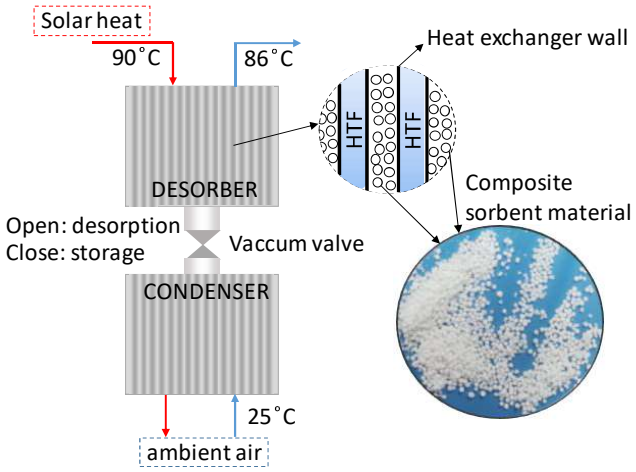

Figure 5. Adsorption heat exchanger in detail.

The performance maps (see Figure 6) provided the charging and discharging power as a function of the adsorber inlet temperature and the condenser or evaporator inlet temperature, respectively. The following mass flow rates were used to obtain the performance maps: 0.2 kg/s in the adsorber, 0.25 kg/s in the condenser, 0.166 kg/s in the evaporator. The calculated maximum stored energy corresponds to 110 MJ per module.

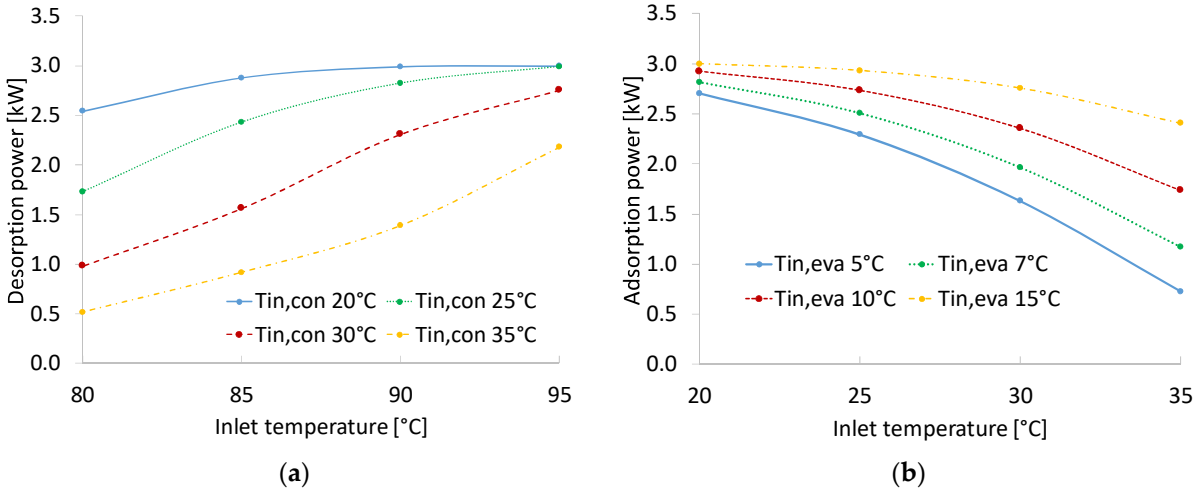

Figure 6. Charging (**a**) and discharging (**b**) performance map of a 100 kg sorption module.

The performance of a sorption system is dependent on the ambient thermal losses between two consecutive charges or discharges. The higher the thermal losses, the more sensible heat will be consumed by the module to reach the regeneration or adsorption temperature again, which negatively impacts on the COP (i.e., the round-trip efficiency of the TES). To calculate the thermal losses, each sorption module was assumed as a lumped system, representing the composite material, the metal heat exchanger, and the HTF. The temperature difference between the module temperature, considered uniform for all the system, and the ambient temperature was the driving force of the heat losses. The sorption storage was assumed to be in a non-heated area of the house or even buried underground. Thus, a constant ambient temperature of 15 °C and 21 °C for winter and summer, respectively, was assumed. In spite of assuming an ambient temperature of 15 °C during winter, a low temperature heat source is required. Otherwise, due to the relatively continuously evaporator heat demand, since the system is located in a closed space, the surrounding temperature would drop down, cooling down the ambient air and thus not being able to provide ambient heat anymore.

Furthermore, a standard insulation of 5 cm of polyurethane, with a thermal conductivity of 0.03 W/m·K, was considered. Under this scenario, the decline of the sorption module was calculated by an exponential decay function, depending on the heat transfer coefficient, calculated based on the natural convection and insulation heat transfer coefficient, an equivalent heat capacity, the total mass of the module, and its external heat transfer area.

Auxiliary elements

The auxiliary subcomponents, the gas boiler, the dry heater, and a buffer water tank (low temperature heat storage) were modelled using state-of-the-art numerical models. The gas boiler was modelled based on the mathematical description used in the type 122 of TRNSYS 18 Documentation [37]. The thermal power (Q) delivered by the dry heater was represented by Equation (3): the equality between the temperature gradient between the inlet and the outlet HTF (water-glycol) temperatures ($T_{out,HTF}$ and $T_{in,HTF}$) and the Fourier's law of heat conduction [38]. The UA value, shown in Equation (3), represents the thermal transmittance of the dry heater heat exchanger per surface area. The UA of the dry heater indicated by the manufacturer [39] under its operating conditions was 320 W/m^{2}K. The maximum thermal power of the boiler and the dry heater considered in the simulations was 9 and 2.75 kW, respectively.

$$Q = \dot{m}\, C_{p,HTF}(T_{out,HTF} - T_{in,HTF}) = UA_{drycooler}(T_{amb} - T_{avg,air}) \quad (3)$$

The water buffer tank that assisted the evaporator during the discharge of the sorption storage was modelled assuming one single control volume of 0.39 m^3 with uniform

temperature. Thermal losses to the ambient were neglected due to its short-term use (some hours).

2.3. Control Description

The system could select between 43 operational modes (described in Appendix A), which consisted in the combination of the operational modes of the solar field, stratified water tank (i.e., combi-tank), sorption storage tank, boiler, and SH supply mode explained in Section 2.1 and presented in Table 3. The operation of the system was controlled by an RBC policy implemented also in Python by the authors of this study. The RBC policy selected an operational mode based on the following system variables: season, solar irradiation, ambient temperature, top and middle temperature of the stratified tank, state of charge of the sorption system, thermal demand, and/or temperature of the low temperature heat storage. The system description presented in Section 2.1 in combination with the simplified RBC policy presented in Appendix A allows to describe the control policy of the system.

Table 3. Operational modes of the system subcomponents.

ID	Action Description	ID	Action Description
Coll_STES	Charge STES with solar heat	DHW_tank	Supply DHW just with combi-tank
Coll_DHW	Charge combi-tank with solar heat for DHW	DHW_boiler	Supply DHW assisted by boiler
Coll_SH	Charge combi-tank with solar heat for SH	SH_tank	Supply SH just with combi-tank
Coll_buffer	Charge buffer-tank with solar heat	SH_boiler	Supply SH assisted by boiler
Dis_STES_buffer	Discharge STES with buffer-tank	SH_closeloop	Supply SH in close loop
Dis_STES_dryheater	Discharge STES with dry heater		

The system under study, which is complex with a large number of operational modes and highly dependent on the weather conditions, required a control optimization to be competitive versus fossil-fuel technologies, which present an easier operation.

Section 2.1 explained that in summer, the sorption modules were charged at high enthalpy solar energy (i.e., >80 °C). Solar heat at lower enthalpy was used to charge the stratified water tank. The same occurred in winter: at relatively high solar irradiation, the system charged the stratified water tank. At low enthalpy solar energy, the low temperature heat storage was charged at around 20 °C. The optimal threshold of solar irradiation at which the operational costs of the system are minimized must be obtained through control optimization. The control threshold to be optimized, which defined the system operation, are:

1. Minimum solar irradiation in summer to charge the sorption storage tank ($G_{MIN,STES}$).
2. Minimum solar irradiation in summer to charge the stratified water tank ($G_{MIN,COMBI,S}$).
3. Minimum solar irradiation in winter to charge the stratified water tank ($G_{MIN,COMBI,W}$).
4. Minimum solar irradiation in winter to charge the low temperature heat source, either PCM tank or buffer water tank ($G_{MIN,LTHS}$).

The control thresholds were optimized with the Hyperopt library [40] of Python. The optimization library was coupled to the RBC policy. In this way, the optimizer provided four different control thresholds to the RBC policy at every iteration. Each iteration consisted in an annual system simulation. Based on those thresholds and the RBC policy, an operational mode was selected, which in turn was given to the system simulation. At the end of the system simulation, the value of the objective function for that iteration was stored. The optimization loop kept running until the optimizer achieved the optimum objective function. The objective function (see Equation (4)) consisted of minimizing the total annual operational costs. This total annual operational cost consisted of the gas and electrical consumption of the system as well as a cost penalty. The penalty was paid each time the SH demand was not supplied. Thus, the control will tend to maintain the middle part of

the stratified water tank as hot as possible to supply SH demand during the periods in which DHW and SH demand are required simultaneously.

$$Annual\ operational\ cost = \sum_{t=0}^{J}\left[PF\ C_{gas}\left(E_{nosup,DHW} + E_{nosup,SH}\right) + C_{gas}E_b + C_{el}E_{el}\right] \quad (4)$$

To calculate the objective function at each annual simulation, the following economic parameters were considered: a penalty factor (*PF*) of unity, a unitary cost for natural gas (C_{gas}) of 61.5 €/MWh, and a unitary cost for electricity (C_{el}) of 298 €/MWh (with taxes) [41] was considered. Furthermore, to calculate the electrical consumption of the dry heater, a ratio of 0.085 [39] between the thermal power rejected from the dry heater and fan electrical power consumption was considered. Eb and Eel represented the gas (at the boiler) and electrical consumption, respectively. Enosup represented the thermal demand that could not be supplied.

2.4. Case Studies

2.4.1. Building Description

The building design (see Figure 7) and construction materials were obtained from the Tabula/Episcope database [42] using the reference building DE.N.SFH.12.Gen reported in a technical report of the SWS-heating European project [43]. The thermal transmittance of the main construction materials is shown in Table 4. The same building design and construction materials were used for all the studied locations. The building model was implemented into OpenStudio Software [44]. The building had two heated thermal zones of 67 m^2 each and a non-heated thermal zone (attic). Using the weather data as input and using a simulation time-step of one hour, the space heating demand of the building for the different climatic files was simulated through EnergyPlus [45]. Each heated thermal zone was divided into living and sleeping areas. The temperature set-points for each thermal zone along the day are presented in Table 5 (obtained from a technical report of the SWS-heating European project [46]). It is important to highlight that the SH temperature set points correspond to a nearly zero-energy building [43], being part of the European Union's goal to move towards zero-emission new buildings by 2030 [47].

Table 4. Thermal transmittance of the construction materials.

Element	External Wall	Floor	Roof	Internal Wall	Ceiling
U [W/m^2K]	0.11	0.12	0.05	1.7	2.9

Table 5. Heating set point schedule.

Description	Heating Schedule	Set Point [°C]
Living area weekday	From 8:00 to 10:00/From 16:00 to 00:00	19
	From 00:00 to 8:00/From 10:00 to 16:00	16
Living area weekend	From 10:00 to 11:00/From 20:00 to 01:00	19
	From 01:00 to 10:00/From 11:00 to 20:00	16
Sleeping area weekday	From 21:00 to 8:00/From 17:00 to 19:00	19
	From 8:00 to 17:00/From 19:00 to 21:00	16
Sleeping area weekend	From 23:00 to 10:00	19
	From 10:00 to 23:00	16

A DHW consumption of 90 l/day [46] with a temperature lift of 50 °K (from 10 to 60 °C) was considered in the simulations. Both the SH and the DHW demand were interpolated to 15 min set-points.

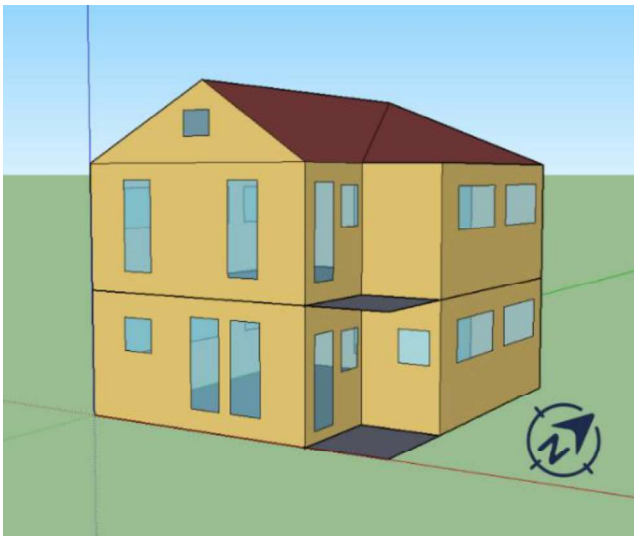

Figure 7. Sketch of the simulated building.

2.4.2. Studied Climates

The thermal performance of a sorption system is highly affected by the climatic conditions, which impact the ambient thermal losses and the availability of the environmental source or sink and of the solar resource. In this study, three different representative cities of central and northern Europe were studied. Paris, Munich, and Stockholm, corresponding to Atlantic, Continental, and Boreal biogeographical regions, respectively, according to the European Environment Agency [48]. According the Köppen climate classification, Paris corresponds to an Oceanic climate (Cfb) and Munich and Stockholm to a Humid Continental Mild Summer (Dfb). Table 6 shows the climatic properties and Table 7 the GPS coordinates and the collector's inclination for each location. To graphically locate the three representative cities, Figure 8 places their position in a map.

Table 6. Location and climatic properties of the studied locations.

City	Climate [19]	Annual $T_{amb,avg}$ [°C]	Winter $T_{amb,avg}$ [°C]	Summer $T_{amb,avg}$ [°C]	Total Annual Titled E_G [kWh/m^2]	Total Summer Titled E_G [kWh/m^2]	Total Winter Titled E_G [kWh/m^2]
Paris	Atlantic	12.5	7.8	17.2	1069	760	309
Munich	Continental	9.4	3.2	15.5	1162	762	400
Stockholm	Boreal	7.8	1.5	14.1	964	728	236

Table 7. GPS coordinates and inclination of solar collectors.

City	Latitude [°]	Longitude [°]	Collector Inclination [°]
Paris	48.817	2.33	35
Munich	48.133	11.7	35
Stockholm	59.35	17.95	45

Meteorological data from Meteonorm [49] for Paris, Munich, and Stockholm were used in the simulations. The meteorological data consisted of average values of the period 1991–2010 with a time-step of 1 h. Figure 9 shows the solar global horizontal irradiation for the three studied locations. All simulations were run in a computer with a 16 GB RAM and an Intel Core i-5 3.30 GHz processor.

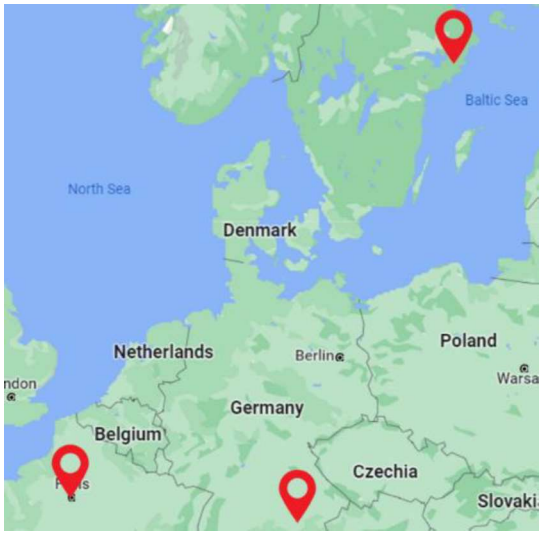

Figure 8. Location of three represented European cities.

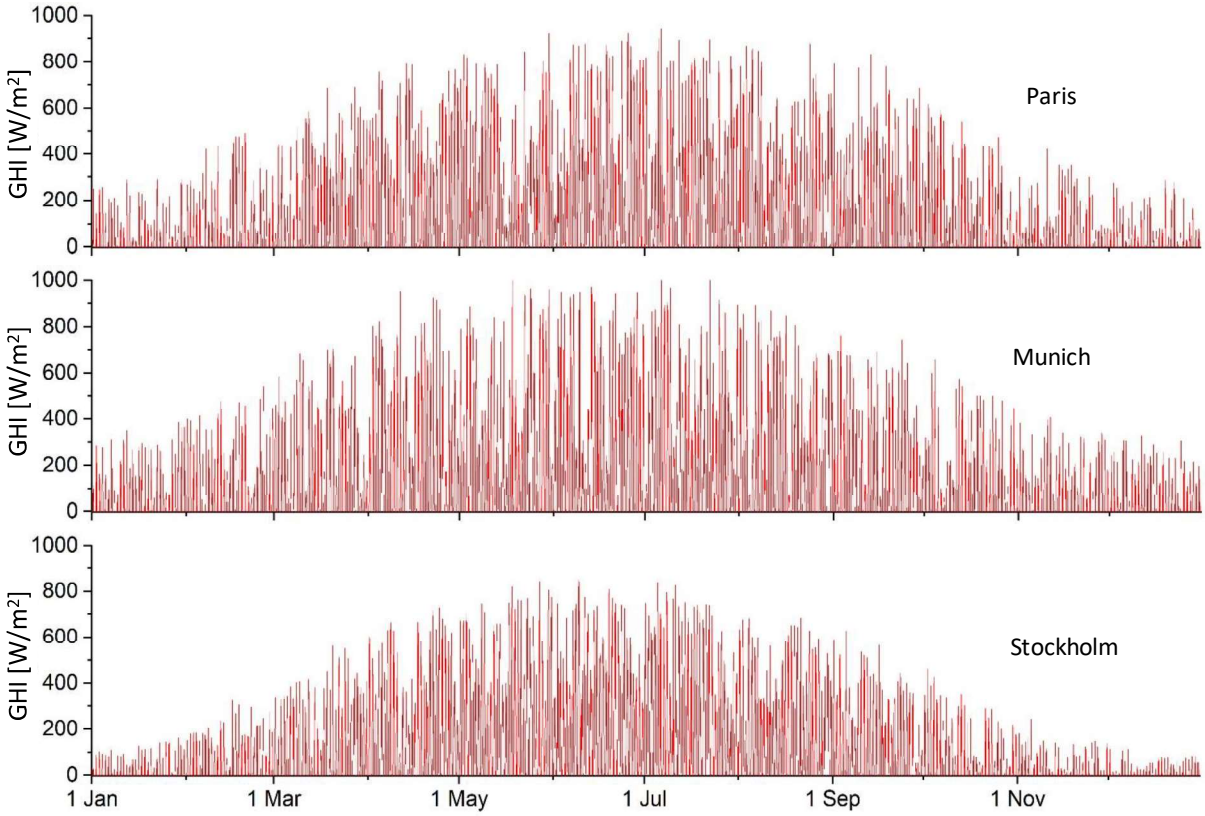

Figure 9. Global horizontal irradiation for the three studied locations.

2.4.3. Key Performance Indicators

For analysis and comparison purposes with other systems, different performance indicators were defined. The thermal performance of the whole solar energy system was evaluated through the solar fraction (*SF*), presented in Equation (5). The solar fraction measures which percentage of the total thermal demand ($D_{DHW} + D_{SH}$) was covered by solar energy, and not by fossil fuels (natural gas in this case). E_b represents in Equation (5) the part of total thermal demand supplied by the gas boiler.

$$SF = \frac{(D_{DHW} + D_{SH}) - E_b}{D_{DHW} + D_{SH}} \quad (5)$$

The thermal performance of a sorption storage system was analysed through the coefficient of performance (COP) and the energy density (e_d), whose numerical definitions are shown in Equations (6) and (7). The COP measures the ratio between the net discharged energy (E_{ad}) versus the total energy required during the charging phase: the sum up of sensible ($E_{de,sen}$) plus sorption (E_{de}) energy. The energy density indicates the net discharged energy versus the volume of the sorbent material.

$$COP = \frac{E_{ad}}{E_{de,sen} + E_{de}} \tag{6}$$

$$e_d = \frac{E_{ad}}{V_{sorb}} \tag{7}$$

The COP summarizes in a single parameter the performance of the sorption storage. Nevertheless, it depends on the charging (η_{ch}) and discharging efficiency (η_{dis}) of the sorption TES. The higher the charging and discharging efficiency, the higher the COP. The charging and discharging efficiency are calculated using the equations:

$$\eta_{ch} = \frac{E_{de}}{E_{de,sen} + E_{de}} \tag{8}$$

$$\eta_{dis} = \frac{E_{ad}}{E_{ad,sen} + E_{ad}} \tag{9}$$

The COP and the energy density have been used by many authors to evaluate the performance of sorption storage systems [10,50,51]. Nevertheless, Fumey et al. [52] reported that performance parameters such as volumetric energy density and volumetric power density are not adequate for comparison due to the highly varying conditions. Those authors proposed a new concept, called temperature effectiveness (TE), which consisted of analysing the ratio of resulting gross temperature lift in sorption (GTL_{ad}), compared to the required temperature lift in desorption (GTL_{de}). The GTL_{ad} depends on the sorption temperature during discharge ($T_{ad,avg}$) and the evaporator temperature ($T_{e,avg}$). On the other side, the GTL_{de} depends on the desorption temperature ($T_{de,avg}$) and the condensing temperature ($T_{c,avg}$) The temperature effectiveness of the STES system under study was calculated using the following equations [52]:

$$TE_{avg} = \frac{GTL_{ad}}{GTL_{de}} \tag{10}$$

$$GTL_{ad} = T_{ad,avg} - T_{e,avg} \tag{11}$$

$$GTL_{de} = T_{de,avg} - T_{c,avg} \tag{12}$$

With regard to the system analysis from an environmental approach, the CO_2 emissions saved by the solar system at each location were analysed. The CO_2 emissions were calculated by multiplying the annual thermal demand supplied by the solar seasonal system, divided by the boiler efficiency (i.e., 0.9), by the equivalent CO_2 emissions (0.18 kg/kWh) [53].

3. Results and Discussion

3.1. Overall System Results

The three studied scenarios were analysed for one year under optimal control policy. Solar irradiation, ambient temperature, and thermal demand of each location have large impacts on the selected system operational mode. The optimal control must search, among other aspects, for the best trade-off between maximum solar heat stored in the sorption system in summer, discharged energy by the sorption system given the winter weather conditions, and solar heat that can be directly supplied to the stratified water tank.

The sorption system temperature decreases due to the thermal losses to the ambient, especially in summer. The longer the intervals between two consecutive charges or discharges, the higher the sensible heat required to reach the regeneration or sorption temperature of the sorbent material, which causes a decrease in the efficiency. From an overall system perspective, during some periods, it may be more efficient and cost-effective to charge the stratified water tank with solar heat than the sorption modules or the low temperature heat source. Hence, the optimal irradiation control thresholds were set to operate the sorption modules only when it was more cost-effective, despite the fact that its full capacity was not exploited.

The optimal control thresholds of the RBC strategy are presented in Table 8. Stockholm was the location with the lowest solar irradiation in winter (see Table 6), but with the highest space heating demand. Especially in this climate, solar heat stored during summer in the sorption system will

be necessary in winter for SH application. Thus, the optimal economic scenario was obtained for a threshold-1 of 421 W/m^2 (see Table 8), a value considerably lower compared to Paris and Munich. This threshold made it possible that in summer, when the solar irradiation was above this value, the sorption system was charged, reaching a maximum state of charge (SoC) of 76% in spite of the lower solar availability. The maximum SoC of the sorption system in Munich, which presented the higher annual total solar irradiation and a thermal demand of 9.88 MWh, was 84 %. The overall system main results for the three studied cities are presented in Tables 9 and 10.

Table 8. Optimal control thresholds.

City	$G_{MIN,STES}$	$G_{MIN,COMBI,S}$	$G_{MIN,COMBI,W}$	$G_{MIN,LTHS}$
Paris [W/m^2]	475	172	115	81
Munich [W/m^2]	464	126	120	80
Stockholm [W/m^2]	421	88	133	82

Table 9. Overall system KPIs for the studied locations.

City	Annual Cost [€]	SF [%]	CO_2 Emissions Savings [kg]	Maximum SoC [%]
Paris	274.9	44.5	576	93.1
Munich	444.8	40.8	808	84.0
Stockholm	706.2	27.0	697	78.2

Table 10. Supplied energy demand and generated solar energy for each location.

City	Total Thermal Demand	Thermal Demand Supplied by System	Thermal Demand Supplied by Boiler	Energy Generated by Solar Field
Paris [MWh]	6.46	2.88	3.58	6.43
Munich [MWh]	9.88	4.04	5.84	7.17
Stockholm [MWh]	12.91	3.48	9.42	5.63

The system obtained solar fractions of 44.5, 40.8, and 27.0% in Paris, Munich, and Stockholm, respectively. The highest solar fraction was reached for Paris due to its higher ratio between total annual solar irradiation (1069 kWh/m^2) and thermal demand (6.46 MWh). The second highest solar fraction was obtained for Munich, which presented higher total annual solar irradiation compared to Paris (8%), but also higher annual thermal demand (9.88 MWh). Stockholm obtained the lowest solar fraction due to its lower solar energy availability (963.8 kW/m^2) and its much higher thermal demand compared to Paris and Munich (2 and 1.3 times more, respectively).

In absolute terms, the solar seasonal system operated under Munich weather conditions supplied the maximum amount of energy to the demand: 4.04 MWh (without fossil fuel support) and therefore saved the maximum amount of CO_2 emissions: 808 kg. The best solar conversion rate (energy generated by the solar field vs. thermal demand supplied by the solar seasonal system) was reached by Stockholm. Its higher space heating in intermediate seasons made it possible to profit better from solar energy.

3.2. Thermal Performance of Sorption Storage

Table 11 presents the KPIs of the sorption storage system for the three studied climates: Paris, Munich, and Stockholm. In the proposed system, the discharge of the sorption modules depended on a low temperature heat source charged by low enthalpy solar heat (see Table 8 for solar irradiation thresholds). Hence, the discharge of the sorption system during winter depended on the solar irradiation. To maximize the system efficiency and minimize the operational costs, the optimal control should choose the scenario in which all the energy stored in the sorption system during summer can be discharged by the end of the winter. The system located in Paris reached the highest charging rate (SoC of 91%). Nevertheless, Paris presented a total winter solar irradiation of 309 kWh/m^2), which could limit the discharging of the sorption system. Nonetheless, thanks to

the high ambient temperatures during winter ($T_{AMB,AVG,W}$ = 7.8 °C) and the use of a dry heater that profits from ambient heat to assist the evaporator, the sorption storage could discharge 91% of its total capacity. In Paris, the dry heater prolonged the discharging of the sorption storage during 112 h per year. The integration of a dry heater to profit ambient heat was explored also under Munich weather conditions. Nevertheless, the dry heater was only used for 9.5 h due to the low ambient temperatures during winter. The few hours of dry-heater operation did not justify its use during winter under climates as Munich or more severe ones. For this reason, in this study the implementation of a dry heater was just considered for Paris. Nonetheless, Munich and Stockholm presented similar sorption storage discharging efficiency (around 69.5%) thanks to the optimization of the system operation.

Table 11. KPIs of the sorption storage system.

City	Use of STES [%]	COP	TE	e_d [kWh/m^3]	$\eta_{CH,\,STES}$ [%]	$\eta_{DIS,\,STES}$ [%]
Paris	91	0.284	0.384	106.2	42.4	69.0
Munich	82	0.277	0.357	96.7	40.8	70.3
Stockholm	76	0.311	0.320	88.5	46.7	68.8

With respect to energy density, Paris reached the highest value with an energy density of 106.2 kWh/m^3. The use of a dry heater, in addition to solar heat, to assist the evaporator during relatively warm winter days allowed to maximize the use of the seasonal sorption system, and in consequence its energy density. Stockholm achieved the best COP because it presented the highest charging efficiency, as will be explained in detail in a further paragraph. Nevertheless, the system operated under Stockholm conditions obtained the lowest energy density (kWh/m^3) due to the lower solar energy availability and the use limitation imposed by the optimized control. In the three locations, the energy densities of the sorption storage were limited by the system operation (maximum used capacity of the STES: 91, 82, and 76%), which aimed to minimize the operational costs. Bearing in mind that the sorption storage had the same size for all the locations, the identification of its maximum used capacity allows to reduce the storage volume and reach higher energy densities for the same climatic area in further designs. For instance, reducing the volume of the sorption storage down to 76% of the original volume, i.e., the optimal size for Stockholm, according to the control optimization, the energy density would increase to a 116.5 kWh/m^3. Nevertheless, this value is lower compared to the values reported for Engel et al. [17] for the same location (Stockholm). For a 6 m^3 of zeolite and 36 m^2 of collectors, the authors obtained energy densities from 156 to 177 kWh/m^3. However, it has to be pointed out that the system was based on zeolite 13X, using much higher regeneration temperature (i.e., above 150 °C), requiring either concentrated solar thermal collectors or power-to-heat process to be efficiently charged.

The temperature effectiveness, introduced by Fumey et al. [52], makes it possible to compare the thermal performance of long-term sorption storage systems in terms of temperature lift. In general, TE is strongly linked to the features of the sorbent material employed, and for this reason, the obtained TEs in the different climatic conditions are quite comparable, with only a slight variation. An average TE for the three studied locations is in line with the values reported in the literature for close fixed systems using solid-sorbent materials, as shown in Table 12. The system under study obtained an average TE of 0.35, which means that relatively low driving temperature (i.e., below 100 °C) is required to charge the system. Indeed, the lowest TEs were obtained for sorption system with desorption temperatures above 150 °C. This means that high effective or concentrated solar collectors are necessary to reach the regeneration temperatures of those systems.

Table 12. TE of different close fixed sorption systems. Adapted from [52].

Author	T_{DE} [°C]	T_{AD} [°C]	GTL_{DE} [°C]	GTL_{AD} [°C]	TE
Finck et al. [14]	103	20	83	30	0.36
Köll et al. [34]	180	45	163	25	0.15
Palomba et al. [15]	90	35	60	25	0.42
Zhao et al. [54]	85	40	67	22	0.33
Jiang et al. [50]	157	58	136	47.4	0.35
Brancato et al. [55]	90	37	60	24.5	0.41
Yan et al. [56]	-	-	154	35	0.23
This study	87.2 *	34.6 *	62.6 *	21.9 *	0.35 *

* Average value for the three studied locations.

To provide a clearer image of the sorption TES performance, Figures 10 and 11 present the sensible energy and sorption energy received by the sorption storage for Paris, Munich, and Stockholm during summer and winter. In the same figures, ambient temperature for the corresponding period was also included since it is very relevant to understand and discuss the results. Solar irradiation for the same time periods can be read in Figure 9. As previously mentioned, the highest COP was obtained for Stockholm, because it presented the highest charging efficiency in spite of its lower solar irradiation during summer compared to Munich and Paris. In fact, having less instantaneous solar power in summer was a benefit, according to the current control. The charging process of the sorption modules in summer works as follows: solar heat is used to raise the temperature of the sorbent material. Once the sorbent material is at the desired regeneration temperature, solar energy around 90 °C charges the sorption storage. During summer days with high solar irradiation, the delivered solar power is much larger than the sorption module can absorb. Therefore, that excess heat is used to increase the temperature of the next sorption module (also avoiding overheating on the solar field). Thus, the module is ready for the sorption process once the active module is fully charged. Nevertheless, if the sorption process of the second module takes a long time to start, that sensible energy provided to prepare the module for the sorption will turn into thermal losses. In Stockholm, the solar irradiation in summer is much lower compared to Munich and Paris. For this reason, less excess solar heat is available to charge the consecutive module. This explains why the charging efficiency of Stockholm is higher: the solar power matched better with the energy required by the active sorption module; therefore, lower thermal losses due to the consecutive module took place. In addition, lower ambient temperatures during charging (i.e., condensation temperature) also increases the performance of the sorption system due to a larger temperature difference between regeneration and condensing temperature.

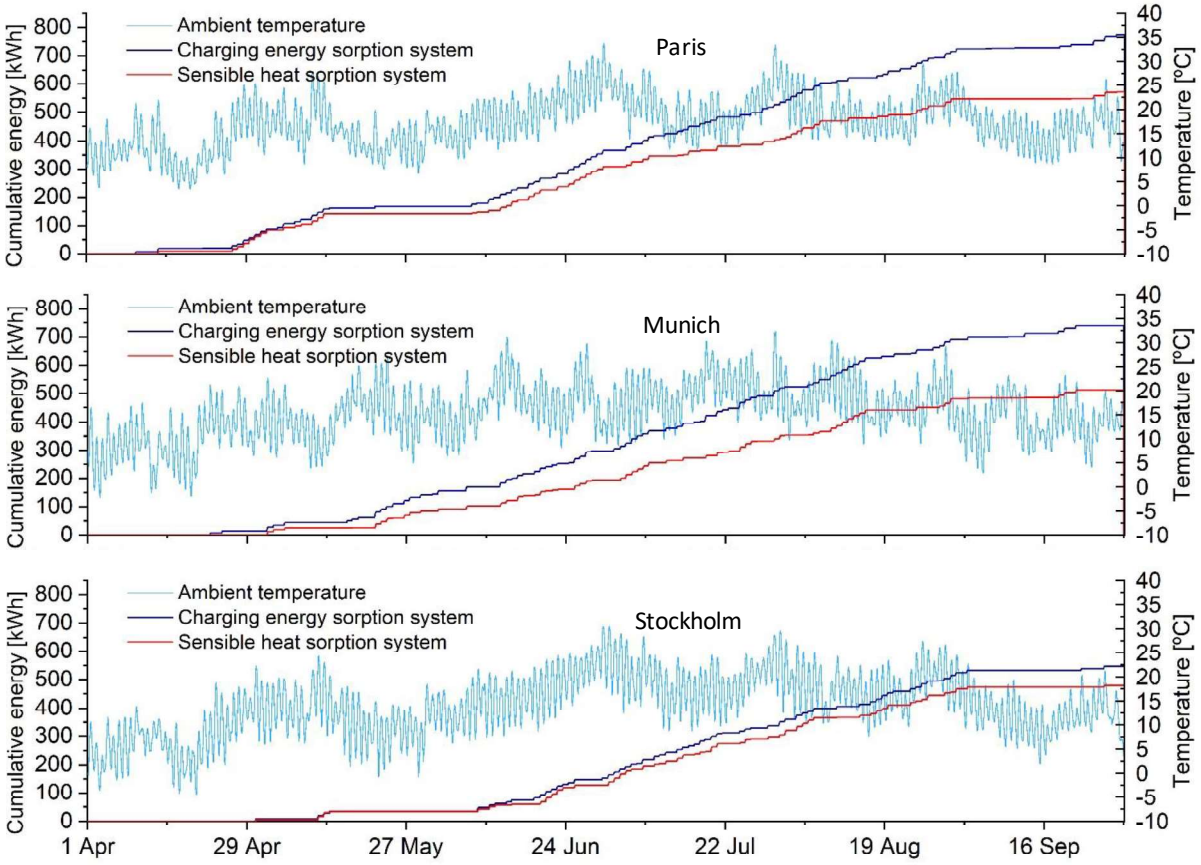

Figure 10. Variables of Paris, Munich, and Stockholm during summer (from April to September).

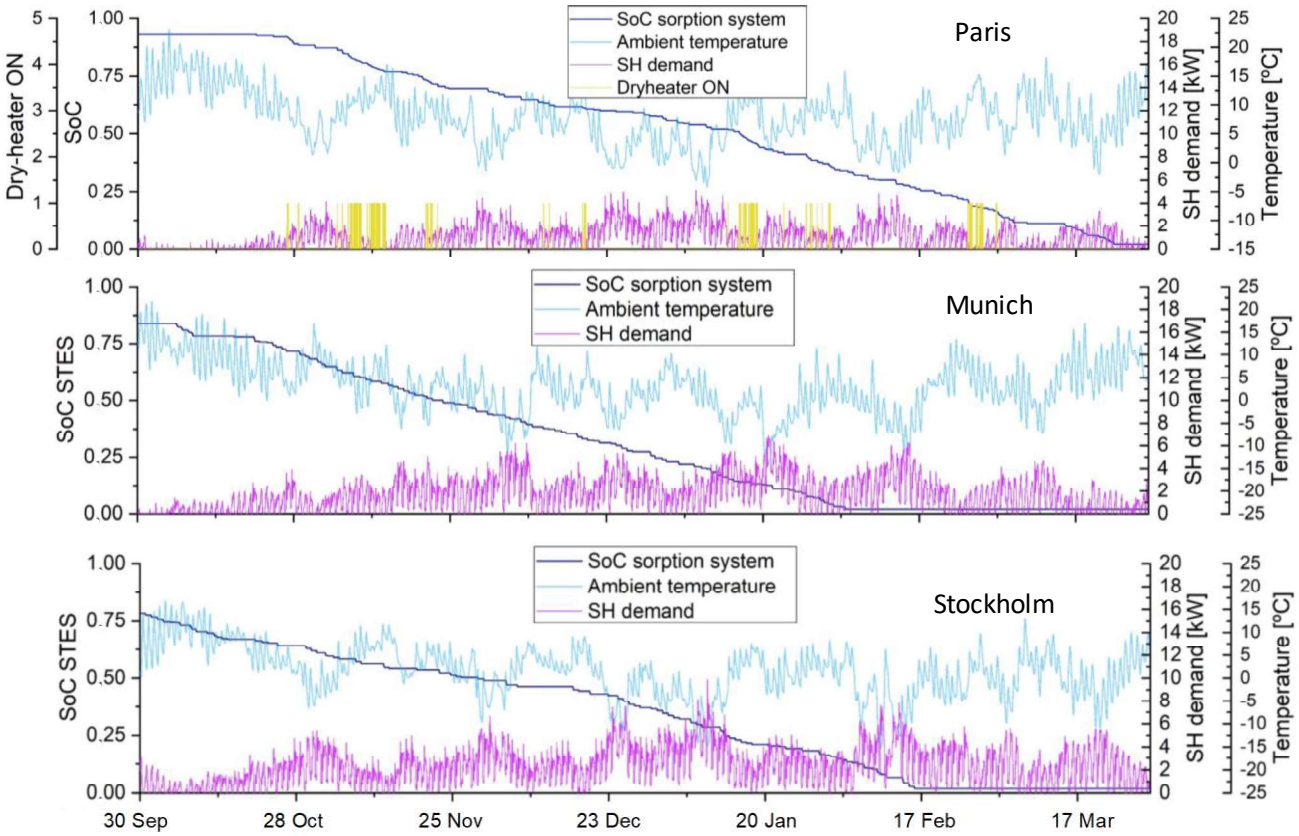

Figure 11. Variables of Paris, Munich, and Stockholm during winter (from October to March).

With respect to the discharging efficiency, the seasonal sorption system located in the three climatic zones presented similar discharging efficiencies. Nevertheless, its operation during winter, presented in Figure 11, was completely different due to the different weather conditions. The sorption TES in Paris required six months, from the beginning of October to the end of March, to be completely discharged. The fastest discharges occurred during the periods when the dry heater could profit from ambient heat. Those days matched with periods of low SH demand. The rest of winter, the sorption TES was discharged roughly continuously, with the exception of a short period in which the low temperature heat storage was not available due to the low solar availability. In Munich, the sorption TES was completely discharged in around four months. Its discharge happened faster due to the following reasons: 1. Higher solar irradiation availability to charge the LTHS compared to Paris and Stockholm; 2. Higher thermal demand at the beginning of the cold season compared to Paris, which required the discharge of the sorption storage. In Stockholm, the energy stored in the sorption storage (72% of the total capacity) was released in 4.5 months. Its discharge was not as continuous as in Munich. During periods with high SH demand, but low solar irradiation, the sorption storage could not be discharged.

As already mentioned, the evaporator of a water-based sorption storage system required heat at a temperature above 0 °C, which was one of the main drawbacks of this type of systems. In the present study, thanks to the use of a low temperature heat source charged by solar energy, the sorption system was discharged at minimum temperatures in winter of −4, −11 and −15 °C (see Figure 11), for Paris, Munich, and Stockholm, respectively, presenting independency from the ambient temperature.

4. Conclusions and Future Perspectives

In this study, the technical performance of a solar-driven water-based sorption system for seasonal storage operated under optimal control policy has been studied for three different climatic zones in central and northern Europe (Paris, Munich, Stockholm). The seasonal energy system composed by 17.5 m^2 of evacuated tube collectors and 3.6 m^3 of SWS reached solar fractions from 28–45% to supply DHW and SH to a single-family house.

The sorption storage system obtained COPs ranging from 0.27 to 0.31. Thanks to an optimal control and its higher charging efficiency, Stockholm obtained the best COP. Stockholm presented low

solar irradiation and high space heating demand in winter. Nevertheless, just 76% of the sorption storage capacity was used in winter, because of the lower solar heat available to drive the evaporator during the discharging phase. The optimal control allowed to identify the sorption storage size that minimizes the system operational costs. None of the three locations used the full capacity of the sorption storage system, which means that the sorption storage size could be reduced for each location in further designs, thus allowing for a reduction of the upfront cost. The optimal RBC strategy based on solar irradiation, ambient temperature, thermal demand, and system state allowed to maximize the competitiveness of the seasonal energy system for each location. Furthermore, the average temperature effectiveness of the sorption storage system was in line with the values of other close systems reported in the literature.

The sorption storage presented independency from ambient temperature during winter thanks to the low temperature heat storage charged by low enthalpy solar heat. The system could operate at minimum temperatures of −15 °C, −11 °C, and −4 °C in Stockholm, Munich, and Paris, respectively. The use of ambient air as a heat source to assist the discharge of the sorption storage was only suitable for an Atlantic climate (Paris), due to its higher ambient temperatures which allowed to provide heat at the minimum temperatures required in the evaporator.

In conclusion, a long-term sorption storage system composed by LiCl/silica gel and driven by solar collectors can be successfully implemented into the heating system of a single-family house in middle and northern Europe, as long as an optimal control based on weather conditions, system state, and thermal demand for each location was carried out. Due to the high system dependency on climatic data and thermal demand, the use of a smart controller that foresees the optimal control operation for each climatic condition may be performed in future studies.

Once the sorption TES concept will be validated in real operating conditions, the future investigation to optimize its operation will need to consider the system from a techno-economic perspective. Similar approaches were recently proposed, for example, for concentrating solar power plants [57], geothermal heat pumps [58], and many other technologies which already reached the right technology readiness level to be considered close to the commercial deployment. Furthermore, the analysis of the social and commercial barriers to increase the acceptability of a new technology like the sorption TES one will need to be undertaken, as recently proposed in [59] for other energy technologies, thus guarantying a rapid market uptake after the development phase will be completed.

Author Contributions: Conceptualization, A.C. and A.d.G.; methodology, A.C., A.d.G. and C.F.; software, A.C. and C.F.; data curation, A.C.; validation, A.C.; formal analysis, A.C.; investigation, A.C.; resources, C.F. and A.d.G.; writing—original draft preparation, A.C.; writing—review and editing, A.d.G., A.F. and C.F.; visualization, A.C.; supervision, A.d.G., C.F. and A.F.; project administration, A.F.; funding acquisition, A.F. All authors have read and agreed to the published version of the manuscript.

Funding: This work was partially funded by the Ministerio de Ciencia, Innovación y Universidades de España (RTI2018-093849-B-C31—MCIU/AEI/FEDER, UE) and by the Ministerio de Ciencia, Innovación y Universidades—Agencia Estatal de Investigación (AEI) (RED2018-102431-T). This work is partially supported by ICREA under the ICREA Academia programme. Alicia Crespo would also like to acknowledge the financial support of the FI-SDUR grant from the AGAUR of the Generalitat de Catalunya and Secretaria d'Universitats i Recerca del Departament d'Empresa i Coneixement de la Generalitat de Catalunya. This work was partially supported by Italian Ministry of University and Research (MUR), program PON R&I 2014/2020—Avviso n. 1735 del 13 July 2017—PNR 2015/2020, under project "NAUSICA—NAvi efficienti tramite l'Utilizzo di Soluzioni tecnologiche Innovative e low CArbon", (ARS01_00334-CUP B45F21000680005).

Institutional Review Board Statement: Not applicable.

Informed Consent Statement: Not applicable.

Data Availability Statement: Data can be provided by the authors upon request.

Acknowledgments: The authors would like to thank Roger Vilà for providing the Meteonorm data. Alvaro de Gracia wants to thank the Serra Hunter Programme for its position at University of Lleida. Alicia Crespo and Cèsar Fernández would like also to thank the Catalan Government for the quality accreditation given to their research group GREiA (2017 SGR 1537). GREiA is a certified agent TECNIO in the category of technology developers from the Government of Catalonia.

Conflicts of Interest: The authors declare no conflict of interest.

Nomenclature

Symbols

C_P	Specific heat, kJ/kgK
$\dot{m}$	Mass flow rate, kg/h
Q	Thermal power, kW
T	Temperature, °C
U	Thermal transmittance, kJ/hm^{2}K
A	Area, m^2
a_0	Collector´s optical efficiency
a_1	First order collector efficiency, W/m^{2}K
a_2	Second order collector efficiency, W/m^{2}K^2
D	Thermal demand, kWh
e_d	Energy density, kWh/m^3
J	Last time-step
t	Time
V	Volume, m^3
E	Energy, kWh
E_G	Solar irradiation, W/m^2
η	Efficiency

Subscripts

b	Boiler
out	Outlet
in	Inlet
avg	Average value
ad	Adsorption
de	Desorption
col	Collector
ch	Charging
e	Evaporator
c	Condenser
sen	Sensible
sorb	Sorbent material
el	Electrical
nosup	Not supplied demand
dis	Discharging
s	Summer
w	Winter
amb	Ambiental
sorb	Sorbent material

Acronyms

SoC	State of charge
SF	Solar fraction
HTF	Heat transfer fluid
PF	Penalty factor
DHW	Domestic hot water
SH	Space heating
COP	Coefficient of performance
GTL	Gross temperature lift
TE	Temperature effectiveness
TES	Thermal energy storage
IAM	Incidence angle modifier of collector
RBC	Rule based control
STES	Seasonal or sorption TES
SWS	Selective water sorbent
LTHS	Low temperature heat source

Appendix A

All possible operational modes to be selected by the RBC policy of the system are shown in Table A1. Figures A1 and A2 depict the simplified RBC policy for summer and winter. Where Dem_sh is the SH demand, Dem_dhw is the DHW demand, SoC_{STES} is the state of charge of the sorption system, Dem_sh_24 h corresponds to the estimated SH thermal demand for the next 24 h, and $T_{combi,top}$ and $T_{combi,middle}$ are the combi-tank temperatures at the top and middle section.

Table A1. System operational modes.

ID	Corresponding Actions	ID	Corresponding Actions
0	No action	22	Coll_SH + SH_closeloop
1	Coll_STES	23	Dis_STES_buffer + SH_closeloop
2	Coll_STES + DHW_tank	24	Coll_buffer
3	Coll_STES + DHW_boiler	25	Coll_buffer + DHW_tank
4	Coll_DHW	26	Coll_buffer + DHW_boiler
5	Coll_DHW + DHW_tank	27	Coll_buffer + SH_tank
6	Coll_DHW + DHW_boiler	28	Coll_buffer +SH_boiler
7	Coll_SH	29	Coll_buffer + SH_closeloop
8	Coll_SH + DHW_tank	30	Coll_DHW + DHW_boiler + SH_tank
9	Coll_DHW + DHW_boiler	31	DHW_boiler + SH_tank
10	Dis_STES_buffer	32	Dis_STES_buffer + DHW_boiler + SH_tank
11	Dis_STES_buffer + DHW_boiler	33	Coll_buffer + DHW_boiler + SH_tank
12	Coll_DHW + SH_tank	34	Dis_STES_buffer + DHW_tank
13	Coll_SH + SH_tank	35 *	Dis_STES_dryheater
14	SH_tank	36 *	Dis_STES_dryheater + DHW_boiler
15	Dis_STES_buffer + SH_tank	37 *	Dis_STES_dryheater + SH_boiler

Table A1. *Cont.*

ID	Corresponding Actions	ID	Corresponding Actions
16	Coll_DHW + SH_boiler	38 *	Dis_STES_dryheater + SH_closeloop
17	Coll_SH + SH_boiler	39 *	Dis_STES_dryheater + DHW_boiler + SH_tank
18	SH_boiler	40	Coll_STES + DHW_tank + SH_tank
19	Dis_STES_buffer + SH_boiler	41	Coll_DHW + DHW_tank + SH_tank
20	SH_closeloop	42	DHW_tank + SH_tank
21	Coll_DHW + SH_closeloop		

* Operational modes only available for Paris.

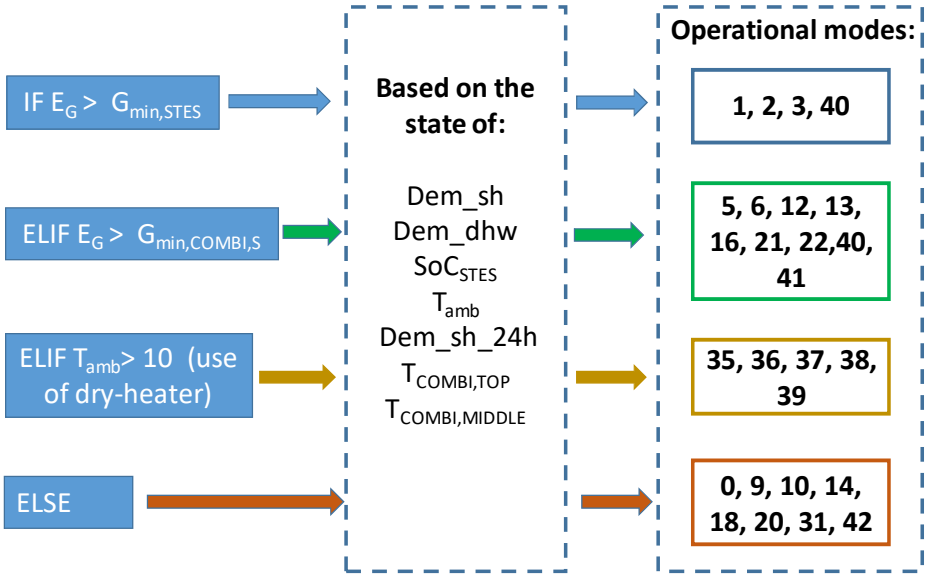

Figure A1. Simplified control policy for summer.

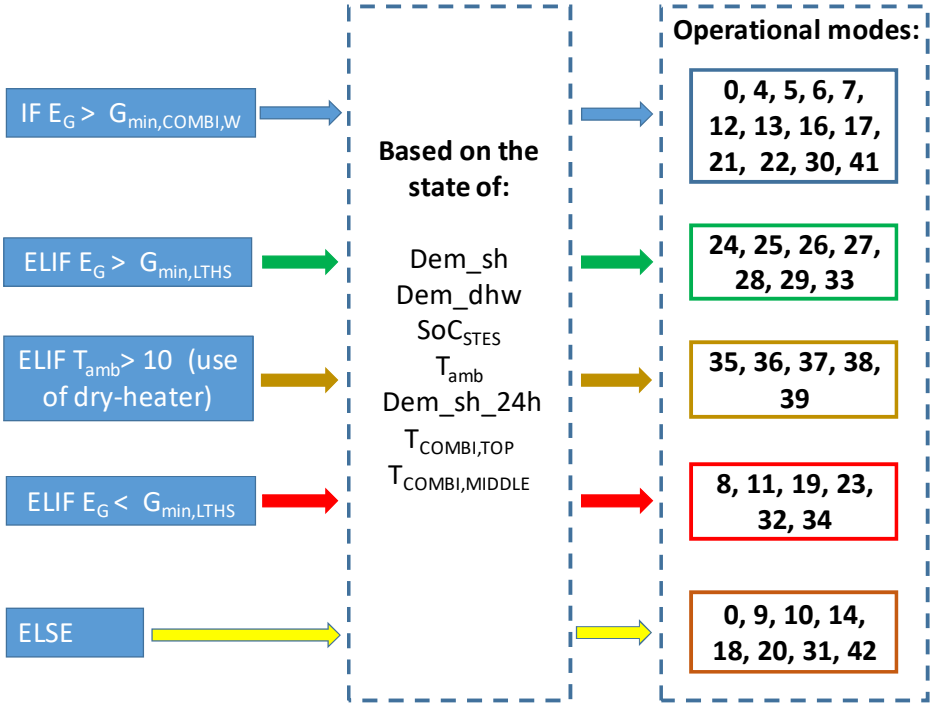

Figure A2. Simplified control policy for winter.

References

1. IEA. *Energy, Climate Change and Environment*; IEA: Paris, France, 2016. Available online: https://www.iea.org/reports/energy-climate-change-and-environment-2016-insights (accessed on 1 May 2022).
2. IEA. *Renewables 2020*; IEA: Paris, France, 2020. Available online: https://www.iea.org/reports/renewables-2020 (accessed on 1 May 2022).
3. IEA. *Heating*; IEA: Paris, France, 2021. Available online: https://www.iea.org/reports/heating (accessed on 1 May 2022).
4. Yang, T.; Liu, W.; Kramer, G.J.; Sun, Q. Seasonal thermal energy storage: A techno-economic literature review. *Renew. Sustain. Energy Rev.* **2021**, *139*, 110732. [CrossRef]
5. Cabeza, L.F. (Ed.) *Advances in Thermal Energy Storage Systems—Methods and Applications*, 2nd ed.; Woodhead Publishing: Cambridgeshire, UK, 2020; ISBN 9780128198858.
6. Frazzica, A.; Freni, A. Adsorbent working pairs for solar thermal energy storage in buildings. *Renew. Energy* **2017**, *110*, 87–94. [CrossRef]
7. Jiang, L.; Liu, W.; Lin, Y.C.; Wang, R.Q.; Zhang, X.J.; Hu, M.K. Hybrid thermochemical sorption seasonal storage for ultra-low temperature solar energy utilization. *Energy* **2022**, *239*, 122068. [CrossRef]
8. Jiang, L.; Li, S.; Wang, R.Q.; Fan, Y.B.; Zhang, X.J.; Roskilly, A.P. Performance analysis on a hybrid compression-assisted sorption thermal battery for seasonal heat storage in severe cold region. *Renew. Energy* **2021**, *180*, 398–409. [CrossRef]
9. Li, T.; Wang, R.; Kiplagat, J.K.; Kang, Y.T. Performance analysis of an integrated energy storage and energy upgrade thermochemical solid-gas sorption system for seasonal storage of solar thermal energy. *Energy* **2013**, *50*, 454–467. [CrossRef]
10. Li, T.X.; Wu, S.; Yan, T.; Wang, R.Z.; Zhu, J. Experimental investigation on a dual-mode thermochemical sorption energy storage system. *Energy* **2017**, *140*, 383–394. [CrossRef]
11. Jähnig, D.; Hausner, R.; Wagner, W.; Isaksson, C. Thermo-chemical storage for solar space heating in a single-family house. In Proceedings of the Ecostock Conference, Galloway, NJ, USA, 31 May–2 June 2006; AEE-INTEC (Austria): Gleisdorf, Austria, 2006; pp. 1–7.
12. Lass-Seyoum, A.; Blicker, M.; Borozdenko, D.; Friedrich, T.; Langhof, T. Transfer of laboratory results on closed sorption thermo-chemical energy storage to a large-scale technical system. *Energy Procedia* **2012**, *30*, 310–320. [CrossRef]
13. Cuypers, R.; Maraz, N.; Eversdijk, J.; Finck, C.; Henquet, E.; Oversloot, H.; Van't Spijker, H.; De Geus, A. Development of a seasonal thermochemical storage system. *Energy Procedia* **2012**, *30*, 207–214. [CrossRef]
14. Finck, C.; Henquet, E.; Van Soest, C.; Oversloot, H.; De Jong, A.J.; Cuypers, R.; Van T'Spijker, H. Experimental results of a 3 kWh thermochemical heat storage module for space heating application. *Energy Procedia* **2014**, *48*, 320–326. [CrossRef]
15. Palomba, V.; Vasta, S.; Freni, A. Experimental testing of AQSOA FAM Z02/water adsorption system for heat and cold storage. *Appl. Therm. Eng.* **2017**, *124*, 967–974. [CrossRef]
16. Ma, Z.; Bao, H.; Roskilly, A.P. Seasonal solar thermal energy storage using thermochemical sorption in domestic dwellings in the UK. *Energy* **2019**, *166*, 213–222. [CrossRef]
17. Engel, G.; Asenbeck, S.; Köll, R.; Kerskes, H.; Wagner, W.; van Helden, W. Simulation of a seasonal, solar-driven sorption storage heating system. *J. Energy Storage* **2017**, *13*, 40–47. [CrossRef]
18. Mlakar, U.; Stropnik, R.; Koželj, R.; Medved, S.; Stritih, U. Experimental and numerical analysis of seasonal solar-energy storage in buildings. *Int. J. Energy Res.* **2019**, *43*, 6409–6418. [CrossRef]
19. Frazzica, A.; Brancato, V.; Dawoud, B. Unified methodology to identify the potential application of seasonal sorption storage technology. *Energies* **2020**, *13*, 1037. [CrossRef]
20. N'Tsoukpoe, K.E.; Kuznik, F. A reality check on long-term thermochemical heat storage for household applications. *Renew. Sustain. Energy Rev.* **2021**, *139*, 110683. [CrossRef]
21. Mikhaeil, M.; Gaderer, M.; Dawoud, B. On the development of an innovative adsorber plate heat exchanger for adsorption heat transformation processes; an experimental and numerical study. *Energy* **2020**, *207*, 118272. [CrossRef]
22. Frazzica, A.; Brancato, V.; Caprì, A.; Cannilla, C.; Gordeeva, L.G.; Aristov, Y.I. Development of "salt in porous matrix" composites based on LiCl for sorption thermal energy storage. *Energy* **2020**, *208*, 118338. [CrossRef]
23. Project report by Ostbayerische Technische Hochschule Regensburg (OTH). Deliverable report 3.1: "*Requirements for the Sysnthesis of Sorbent Materials*" of the EU H2020 project SWS-Heating. 2018.
24. Van Rossum, G.; Drake, F.L., Jr. *Python Reference Manual*; Centrum voor Wiskunde en Informatica: Amsterdam, The Netherlands, 1995.
25. Project report by Ostbayerische Technische Hochschule Regensburg (OTH). Deliverable report 2.4: "*Key Design and Sizing Features of the Generic Heating System*" of the EU H2020 project SWS Heating. 2019.
26. Collector OEM Vario 3000-30 hp. AkoTec Produktionsgesellschaft GmbH. Available online: https://www.akotec.eu/ (accessed on 1 May 2020).
27. Duffie, J.A.; Beckamnn, W.A. *Solar Engineering of Thermal Processes*, 4th ed.; John Wiley & Sons, Inc: Hoboken, NJ, USA, 2013; ISBN 9780470873663.
28. Project report by University of Lleida; National Technical University of Athens; Istituto di Tecnologie Avanzate per l'Energia. Deliverable report 5.1: "Optimised system control and strategies" of the EU H2020 project SWS-Heating. 2020.
29. TÜVRheinland. *Solar KEYMARK Certificate—Licence Number: 011-7S660R of the Collector OEM Vario 3000-30 hp of Akotec Produktionsgesellschaft GmbH*; TÜV Rheinland: Cologne, Germany, 2013.

30. Ayompe, L.M.; Duffy, A.; Mccormack, S.J.; Conlon, M. Validated TRNSYS model for forced circulation solar water heating systems with fl at plate and heat pipe evacuated tube collectors. *Appl. Therm. Eng.* **2011**, *31*, 1536–1542. [CrossRef]
31. Rodríguez-Hidalgo, M.C.; Rodríguez-Aumente, P.A.; Lecuona, A.; Legrand, M.; Ventas, R. Domestic hot water consumption vs. solar thermal energy storage: The optimum size of the storage tank. *Appl. Energy* **2012**, *97*, 897–906. [CrossRef]
32. Vérez, D.; Borri, E.; Crespo, A.; Zsembinszki, G.; Dawoud, B.; Cabeza, L.F. Experimental study of a small-size vacuum insulated water tank for building applications. *Sustainability* **2021**, *13*, 5329. [CrossRef]
33. Sirch Tankbau-Tankservice Speicherbau GmbH. Available online: https://pufferspeicher-sirch.de/start/ (accessed on 14 September 2021).
34. Köll, R.; Van Helden, W.; Engel, G.; Wagner, W.; Dang, B.; Jänchen, J.; Kerskes, H.; Badenhop, T.; Herzog, T. An experimental investigation of a realistic-scale seasonal solar adsorption storage system for buildings. *Sol. Energy* **2017**, *155*, 388–397. [CrossRef]
35. Hu, P.; Wang, S.; Wang, J.; Jiang, S.; Sun, Y.; Ma, Z. Scale-up of open zeolite bed reactors for sorption energy storage: Theory and experiment. *Energy Build.* **2022**, *264*, 112077. [CrossRef]
36. Brancato, V.; Frazzica, A.; Caprì, A.; Gordeeva, L.; Aristov, Y.; Mikhaeil, M.; Dawoud, B. SWS composites based on LiCl for sorption thermal energy storage: Thermochemical and kinetic properties. In Proceedings of the ENERSTOCK, Ljubljana, Slovenia, 9–11 June 2021.
37. Klein, S.A. 2017, TRNSYS 18: A Transient System Simulation Program, Solar Energy Laboratory, University of Wisconsin, Madison, USA. Documentation: *Volume 4—Mathematical Reference—Type 122: Boiler*. Available online: http://sel.me.wisc.edu/trnsys (accessed on 30 June 2022).
38. Holman, J.P. *Heat Transfer*, 10th ed.; McGraw-Hill Education: New York, NY, USA, 2009; ISBN 978-0073529363.
39. Roen Est Group. Available online: https://www.roenest.com/download/ (accessed on 10 November 2021).
40. Shevchuk, Y. NeuPy—Neural Networks in Python. Available online: http://neupy.com/2016/12/17/hyperparameter_optimization_for_neural_networks.html#tree-structured-parzen-estimators-tpe (accessed on 2 February 2021).
41. Bundesnetzagentur; Bundeskartellamt. Monitoring Report 2017—Key Findings. Technical Report. Available online: https://www.bundesnetzagentur.de/ (accessed on 1 April 2020).
42. IEE Project TABULA. Institut Wohnen und Umwelt GmbH (IWU) and Partners (2009–2012). Available online: https://episcope.eu/iee-project/tabula/ (accessed on 18 April 2021).
43. University of Perugia. Definition of climatic and building typologies boundary conditions. In *Deliverable Report 2.1 of SWS-Heating H2020 European Project*; Universidad de Lleida: Lleida, Spain, 2018.
44. Guglielmetti, R.; Macumber, D.; Long, N. OpenStudio: An Open Source Integrated Analysis Platform. In Proceedings of the Proceedings of Building Simulation, Sydney, Australia, 14–16 November 2011.
45. Crawley, D.B.; Lawrie, L.K.; Winkelmann, F.C.; Buhl, W.F.; Huang, Y.J.; Pedersen, C.O.; Strand, R.K.; Liesen, R.J.; Fisher, D.E.; Witte, M.J.; et al. EnergyPlus: Creating a new-generation building energy simulation program. *Energy Build.* **2001**, *33*, 319–331. [CrossRef]
46. Project report by University of Perugia. Deliverable report 5.3: "Dynamic user-building interaction model predicting thermal-energy behaviour" of the EU H2020 ProjectSWS-Heating. 2019.
47. IEA. *Tracking Buildings 2021*; IEA: Paris, France, 2021. Available online: https://www.iea.org/reports/tracking-buildings-2021 (accessed on 1 May 2022).
48. European Environment Agency. Biogeographic Regions in Europe. Available online: https://www.eea.europa.eu/data-and-maps/figures/biogeographical-regions-in-europe-1 (accessed on 15 April 2022).
49. Meteonorm Software. Available online: https://meteonorm.com/en/ (accessed on 1 April 2022).
50. Jiang, L.; Wang, R.Z.; Wang, L.W.; Roskilly, A.P. Investigation on an innovative resorption system for seasonal thermal energy storage. *Energy Convers. Manag.* **2017**, *149*, 129–139. [CrossRef]
51. Bau, U.; Hoseinpoori, P.; Graf, S.; Schreiber, H.; Lanzerath, F.; Kirches, C.; Bardow, A. Dynamic optimisation of adsorber-bed designs ensuring optimal control. *Appl. Therm. Eng.* **2017**, *125*, 1565–1576. [CrossRef]
52. Fumey, B.; Weber, R.; Baldini, L. Sorption based long-term thermal energy storage—Process classification and analysis of performance limitations: A review. *Renew. Sustain. Energy Rev.* **2019**, *111*, 57–74. [CrossRef]
53. Catalan Office of Climate Change. Practical Guide for Calculating Greenhouse has (ghg) Emissions. Available online: https://canviclimatic.gencat.cat/web/.content/04_ACTUA/Com_calcular_emissions_GEH/guia_de_calcul_demissions_de_ca/190301_Practical-guide-calculating-GHG-emissions_OCCC.pdf (accessed on 1 April 2022).
54. Zhao, Y.J.; Wang, R.Z.; Li, T.X.; Nomura, Y. Investigation of a 10 kWh sorption heat storage device for effective utilization of low-grade thermal energy. *Energy* **2016**, *113*, 739–747. [CrossRef]
55. Brancato, V.; Gordeeva, L.G.; Sapienza, A.; Palomba, V.; Vasta, S.; Grekova, A.D.; Frazzica, A.; Aristov, Y.I. Experimental characterization of the LiCl/vermiculite composite for sorption heat storage applications. *Int. J. Refrig.* **2019**, *105*, 92–100. [CrossRef]
56. Yan, T.; Wang, R.Z.; Li, T.X. Experimental investigation on thermochemical heat storage using manganese chloride/ammonia. *Energy* **2018**, *143*, 562–574. [CrossRef]
57. Tahir, S.; Ahmad, M.; Abd-ur-Rehman, H.M.; Shakir, S. Techno-economic assessment of concentrated solar thermal power generation and potential barriers in its deployment in Pakistan. *J. Clean. Prod.* **2021**, *293*, 126125. [CrossRef]

58. Zhou, K.; Mao, J.; Zhang, H.; Li, Y.; Yu, X.; Chen, F.; Li, M. Design strategy and techno-economic optimization for hybrid ground heat exchangers of ground source heat pump system. *Sustain. Energy Technol. Assess.* **2022**, *52*, 102140. [CrossRef]
59. Andal, A.G.; PraveenKumar, S.; Andal, E.G.; Qasim, M.A.; Velkin, V.I. Perspectives on the Barriers to Nuclear Power Generation in the Philippines: Prospects for Directions in Energy Research in the Global South. *Inventions* **2022**, *7*, 53. [CrossRef]